

Article

Bioactive Carbonate Apatite Cement with Enhanced Compressive Strength via Incorporation of Silica Calcium Phosphate Composites and Calcium Hydroxide

Arief Cahyanto ^{1,2,3,*} , Michella Liemidia ⁴, Elin Karlina ^{1,2}, Myrna Nurlatifah Zakaria ^{2,5} ,
Khairul Anuar Shariff ⁶ , Cortino Sukotjo ^{7,*}  and Ahmed El-Ghannam ⁸

¹ Department of Dental Materials Science and Technology, Faculty of Dentistry, Padjadjaran University, Jl. Raya Bandung Sumedang KM 21, Jatinangor 45363, Indonesia

² Department of Restorative Dentistry, Faculty of Dentistry, University of Malaya, Kuala Lumpur 50603, Malaysia

³ Biomaterials Technology Research Groups, Faculty of Dentistry, University of Malaya, Kuala Lumpur 50603, Malaysia

⁴ Faculty of Dentistry, Padjadjaran University, Jl. Raya Bandung Sumedang KM 21, Jatinangor 45363, Indonesia

⁵ Department of Endodontology and Operative Dentistry, Faculty of Dentistry, Universitas Jenderal Achmad Yani, Jl. Terusan Jenderal Sudirman, Cimahi 40531, Indonesia

⁶ School of Materials and Mineral Resources Engineering, Engineering Campus, Universiti Sains Malaysia, Nibong Tebal, Pulau Pinang 14300, Malaysia

⁷ Department of Restorative Dentistry, University of Illinois at Chicago, Chicago, IL 60612, USA

⁸ Department of Mechanical Engineering and Engineering Science, University of North Carolina at Charlotte, Charlotte, NC 28223, USA

* Correspondence: arief.cahyanto@unpad.ac.id (A.C.); csukotjo@uic.edu (C.S.)

Abstract: Carbonate apatite (CO₃Ap) is a bioceramic material with excellent properties for bone and dentin regeneration. To enhance its mechanical strength and bioactivity, silica calcium phosphate composites (Si-CaP) and calcium hydroxide (Ca(OH)₂) were added to CO₃Ap cement. The aim of this study was to investigate the effect of Si-CaP and Ca(OH)₂ on the mechanical properties in terms of the compressive strength and biological characteristics of CO₃Ap cement, specifically the formation of an apatite layer and the exchange of Ca, P, and Si elements. Five groups were prepared by mixing CO₃Ap powder consisting of dicalcium phosphate anhydrous and vaterite powder added by varying ratios of Si-CaP and Ca(OH)₂ and 0.2 mol/L Na₂HPO₄ as a liquid. All groups underwent compressive strength testing, and the group with the highest strength was evaluated for bioactivity by soaking it in simulated body fluid (SBF) for one, seven, 14, and 21 days. The group that added 3% Si-CaP and 7% Ca(OH)₂ had the highest compressive strength among the groups. SEM analysis revealed the formation of needle-like apatite crystals from the first day of SBF soaking, and EDS analysis indicated an increase in Ca, P, and Si elements. XRD and FTIR analyses confirmed the presence of apatite. This combination of additives improved the compressive strength and showed the good bioactivity performance of CO₃Ap cement, making it a potential biomaterial for bone and dental engineering applications.

Keywords: compressive strength; bioactivity; carbonate apatite; silica calcium phosphate composite; calcium hydroxide; SBF



Citation: Cahyanto, A.; Liemidia, M.; Karlina, E.; Zakaria, M.N.; Shariff, K.A.; Sukotjo, C.; El-Ghannam, A. Bioactive Carbonate Apatite Cement with Enhanced Compressive Strength via Incorporation of Silica Calcium Phosphate Composites and Calcium Hydroxide. *Materials* **2023**, *16*, 2071. <https://doi.org/10.3390/ma16052071>

Academic Editor: Agata Przekora-Kuśmierz

Received: 1 January 2023

Revised: 28 February 2023

Accepted: 2 March 2023

Published: 3 March 2023



Copyright: © 2023 by the authors. Licensee MDPI, Basel, Switzerland. This article is an open access article distributed under the terms and conditions of the Creative Commons Attribution (CC BY) license (<https://creativecommons.org/licenses/by/4.0/>).

1. Introduction

Calcium phosphate cement is a bioactive bioceramic commonly studied as a bone substitute [1,2]. It has the ability to release calcium ions to its surface, providing a chemical bond to the hydroxyapatite structure of the bone, creating a good seal between the cement and bone [2–4]. The ability of this cement to form carbonate apatite (CO₃Ap), with physical and chemical properties similar to bone mineral composition, its high solubility to be replaced with natural bone cells, and its capacity for osteogenesis, also make them a potential

material for dentin-pulp regeneration. Recent research has shown that CO₃Ap cement and Si-CaP in medical and dental applications have increased due to their unique properties, including biocompatibility and chemical similarity to natural bone [2,4,5]. In vivo studies showed that the material could create a physiological environment in the presence of blood from the pulp and induce dentinogenesis [3,6]. However, the most significant drawback of such bioceramics is the poor mechanical properties. This issue has been addressed through the development and incorporation of bioglass into the cement [7–9].

Silica in silica calcium phosphate composite (Si-CaP) can increase the material's mechanical properties by establishing chemical bonding, which provides stability [6,9]. Si-CaP displayed a release of Si⁴⁺ and PO₄³⁻ ions to its surroundings and contributed to osteoblasts' maturation and hydroxyapatite formation on the surface layer [10,11]. On the other hand, calcium hydroxide [Ca(OH)₂], a well-documented material in endodontics due to its superior antimicrobial property and the ability to induce dentinal bridge barrier on an exposed pulp, is also a good calcium ions provider. Ca(OH)₂ works through the dissociation of Ca²⁺ and OH⁻ when in contact with water, elevating the alkalinity of the environment, resulting in a fatal effect on bacteria and stimulating the recruitment, proliferation, and activation of stem cells, undifferentiated cells, and odontoblast from the pulp to form reparative dentin. Long-term and meta-analytical studies have reported its superior use as a vital pulp therapy material [12]. Adding Ca(OH)₂ to CO₃Ap cement could benefit the cement's biological properties. However, consideration must be taken as it could also weaken the mechanical properties of the cement.

The mechanical and bioactivity of CO₃Ap cement are essential factors in the fabricating and synthesizing biomaterials. These materials have been found to promote bone growth and regeneration, making them ideal for use in various clinical applications [2]. Additionally, their ability to integrate with existing bone tissue has improved patient outcomes and reduced the need for additional surgeries. While CO₃Ap and Si-CaP have been widely used in dental and medical applications due to their biocompatibility and similarity to natural bone, there have been concerns regarding their mechanical properties. Incorporating bioglass into the cement has been a solution to address this issue, but there is still a need to improve the mechanical properties and bioactivity of these materials for better clinical outcomes.

The bioactivity of these materials has been attributed to their compositional and surface characteristics. However, little is known about the interactions between the constituent minerals and the overall properties of the composites. Bioactive substances are brought into contact with the body's fluids, and apatite begins to form on the surface of the bone. Evidence of a chemical bond between the material and the tissue can be seen in the formation of an apatite layer on the contacted tissue [13,14]. The release of Ca²⁺ and PO₄³⁻ ions initiate apatite layer formation due to external pH changes [15]. In addition, the release of Ca²⁺ and PO₄³⁻ ions plays an essential part in the tissue regeneration process and dentinogenesis or dentin-pulp regeneration [2]. The in vitro evaluation of cement's ability to form an apatite layer can be carried out using a medium that simulates body fluid developed by Kokubo with ion concentrations similar to the body plasma [16,17].

We look at the potential properties of Ca(OH)₂ to increase the Ca element of CO₃Ap cement. However, concern also arises about compromising its mechanical properties. Therefore, the addition of Si-CaP could be a solution to overcome this issue while at the same time potentially enhancing the bioactivity. In this study, we investigate the mechanical property in terms of the compressive strength and bioactivity of CO₃Ap cement incorporated with Si-CaP and Ca(OH)₂ to form an apatite layer. We hypothesize that incorporating Si-CaP and Ca(OH)₂ into CO₃Ap cement will improve its compressive strength and show good bioactivity performance.

2. Materials and Methods

2.1. Preparation Specimen Groups

Vaterite and dicalcium phosphate anhydrous (DCPA) were utilized as a precursor for CO₃Ap. Vaterite was synthesized according to the previous study (9). The DCPA (J.T. Baker Chemical Co., Phillipsburg, NJ, USA) and Ca(OH)₂ (Emsure Millipore Corp., Burlington, MA, USA) powders were used without further processing. Si-CaP used in this study consists of 19.49% SiO₂, 20.34% P₂O₅, 40.68% CaO, and 19.49% Na₂O (in mol %) [18].

The cement powder was divided into one control group and five test groups. For the control group, a combination of only 60% DCPA and 40% vaterite were employed [19]. Each group has a similar composition for 60% DCPA and 30% vaterite but differs in the weight percentage of the addition of Si-CaP and Ca(OH)₂, as shown in Table 1. All vaterite, DCPA, Si-CaP, and Ca(OH)₂ powders were mixed homogeneously to obtain cement powder. The prepared powders specimen was manipulated with 0.2 mol/L of disodium hydrogen phosphate (Na₂HPO₄; pH 8.2) supplemented with κ-Carrageenan (Sigma-Aldrich, Singapore, Singapore), a hydrosoluble polymer for the cement liquid to form a homogenous cement.

Table 1. The powder composition specimens.

Groups	Powder Compositions	Additional Powder
Control	60% DCPA and 40% vaterite	
1		0% Si-CaP and 10% Ca(OH) ₂
2		3% Si-CaP and 7% Ca(OH) ₂
3	60% DCPA and 30% vaterite	5% Si-CaP and 5% Ca(OH) ₂
4		7% Si-CaP and 3% Ca(OH) ₂
5		10% Si-CaP and 0% Ca(OH) ₂

The compressive strength of the paste was evaluated by filling a Teflon mold with a diameter of 4 mm and a height of 6 mm following the ISO 7489:19868 (ISO 9917:1991 reference) standard. This standard involves preparing cement specimens in a mold and allowing them to be set under controlled conditions. The standard also specifies the compressive strength test's testing conditions, including the specimens' size and shape, the loading rate, and the temperature and humidity conditions during testing. These testing conditions are critical to ensure the accuracy and consistency of the test results, which is essential to ensure that the cement is reliable and suitable for its intended clinical applications. Powder and liquid phases had a liquid-to-powder (L/P) ratio of 0.4. The L/P ratio of 0.4 was the optimized L/P ratio determination through experiments and based on clinical expert assessment.

For the bioactivity evaluation, specimens were prepared in a Teflon mold with a diameter of 10 mm and a height of 2 mm, following the ISO 23317 standard [20]. This standard provides a method for testing the ability of materials to form a layer of apatite in simulated body fluid (SBF). The formation of apatite on the surface of an implant material indicates its ability to integrate with surrounding bone tissue and promote osseointegration. The test involves immersing the material in SBF for a specific time under controlled conditions. SBF is designed to mimic the ionic composition and pH of human blood plasma and promote apatite formation on the material's surface. Following immersion in SBF, the material is analyzed for the presence of apatite using techniques, such as X-ray diffraction, scanning electron microscopy, or energy-dispersive X-ray spectroscopy. The analysis results are used to determine the extent and quality of apatite formation on the material's surface.

Both ends of the mold were covered by glass slides and clamped by a metal clip. The molds were then stored in a container with distilled water to maintain 100% relative humidity and placed into an incubator at 37 °C for 72 h. After incubation, specimens

were removed from the molds, immersed in 99% ethanol for 3 min, and dried in an oven at 80 °C for 3 h.

2.2. Compressive Strength Measurement

The set specimens were subjected to a compressive strength test to evaluate its mechanical strength. The compressive strength is evaluated by the maximum force applied when the specimen fractures and calculates the compressive strength value (C) in MegaPascals (MPa) using the below equation:

$$C = 4p/\pi d^2$$

where

p is the maximum force applied, in Newtons (N);

d is the measured diameter of the specimen, in millimeters (mm).

Ten specimens were used for each group, and the mean compressive strength value was used as data. The specimens were crushed using a universal testing machine (Lloyd Instruments Ltd., West Sussex, UK) with 5.6 N load stress at a 1 mm/min crosshead speed. The 5.6 N load stress was employed to apply force to the specimens and measure their resistance to compressive deformation. The inclusion criteria of the compressive strength specimen measurement were specimens that meet specific size and shape requirements, specimens free from visible cracks or defects, and specimens set after 72 h and ready for testing. Meanwhile, the exclusion criteria of the compressive strength specimen measurement were specimens with visible cracks or defects, specimens not fully set even after 72 h, and specimens not the correct size or shape for testing.

2.3. Preparation and Calculation of SBF

The SBF was prepared by Bogor Botanical Institute, Bogor, Indonesia, according to ISO 23317. The volume of SBF was calculated using the following equation: $v_s = S_a/10$, where v_s is the volume of the SBF (mm³) and S_a is the apparent surface area of the specimen (mm²). The calculated SBF (21.89 mL) was kept in an enclosed bottle and maintained at 36.5 °C.

2.4. Bioactivity Evaluation Procedure

The group with the highest compressive strength was further evaluated for its bioactivity. The specimens were soaked into the SBF for 21 days, and the SBF solution was replaced twice weekly and evaluated at four different periods: 1, 7, 14, and 21 day(s) [11]. In each evaluation time, the specimens were taken from the SBF, gently rinsed with pure water, and then dried in a desiccator at room temperature for further analysis.

2.5. Scanning Electron Microscope and Energy Dispersive Spectroscopy (SEM-EDS)

The CO₃Ap- Si-CaP -Ca(OH)₂ specimen was coated with gold using a sputtering machine. Then, SEM at 15 kV accelerating voltage and EDS were used to examine the microstructure of the surface as well as the mass % of Ca, P, and Si elements (JEOL JSM-G510A, Tokyo, Japan).

2.6. X-ray Diffraction (XRD)

Set CO₃Ap- Si-CaP -Ca(OH)₂ cement specimens were ground to obtain fine powder for XRD analysis. Specimen powder was examined by XRD machine (D2 Phaser, Bruker Corp., Billerica, MA, USA) in the range of 3°–50° in 2 theta (θ) using CuK α ($\lambda = 0.15405$ nm) radiation operated at 40 kV of tube voltage and 40 mA of tube current.

2.7. Fourier-Transform Infrared (FTIR)

The evaluation of the FTIR (Spectrum 100, Perkin Elmer Inc., Shelton, CT, USA) was performed using the KBr method. The KBr and CO₃Ap- Si-CaP -Ca(OH)₂ fine powder at a 200:1 ratio was mixed homogeneously, and the compacted pellets were put in a stainless

steel die. A spectral resolution of 4 cm^{-1} and a range of wavelengths from $400\text{--}4000\text{ cm}^{-1}$ were used to investigate the chemical structural changes.

2.8. Statistical Analysis

KaleidaGraph 4.1 (Synergy Software, Reading, PA, USA) was used to perform one-way factorial ANOVA with Fisher's LSD method as a post hoc test on data relevant to compressive strength. The level of statistical significance was chosen at $p < 0.05$.

3. Results

3.1. Compressive Strength Evaluation

Figure 1 summarizes the compressive strength of the specimens after setting in 100% relative humidity at $37\text{ }^\circ\text{C}$ for 72 h. The compressive strength of the cement specimens varied significantly among the six groups. Group 2 exhibited the highest strength at $23.97 \pm 4.46\text{ MPa}$; this difference was statistically significant compared to all other groups (*; $p < 0.05$). This indicates that the properties of the cement in Group 2 were notably different and most resistant to compression. On the other hand, Group 3 had the lowest compressive strength at $11.05 \pm 5.92\text{ MPa}$ and this difference was also statistically significant compared to the other groups, indicating that the cement in this group was the least resistant to compression. Additionally, it is noteworthy that there was a statistically significant (**; $p < 0.05$) difference between Group 1 and Groups 3 and 4, with Group 1 exhibiting higher compressive strength than Groups 3 and 4, indicating different properties of the cement in Group 1 compared to those in Groups 3 and 4.

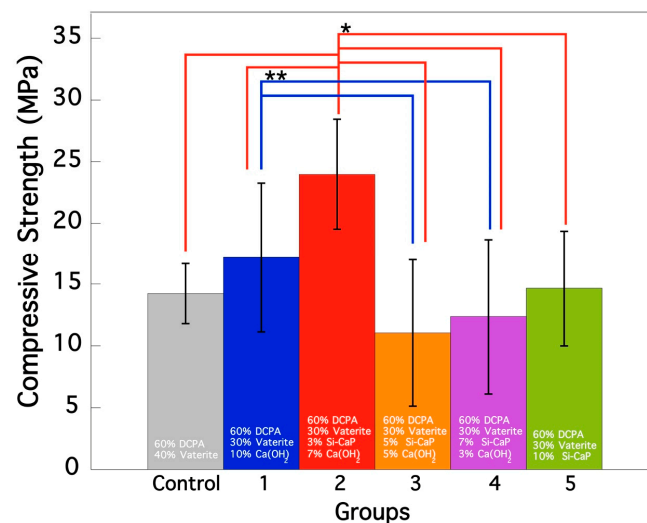


Figure 1. Compressive strength evaluation of CO_3Ap -Si-CaP- $\text{Ca}(\text{OH})_2$ cement specimens after 72 h of treatment. Ten specimens of each group were measured for compressive strength, and error bars indicate the standard deviation. Symbols of * and ** were showed statistically significant between the groups.

Regarding the comparison between the control group and Group 1, the results showed a slight improvement in compressive strength in Group 1 compared to the control group. However, the difference between the mean values of the two groups was not statistically significant ($p > 0.05$). This suggests that the addition of $\text{Ca}(\text{OH})_2$ alone did not significantly improve the compressive strength of the cement. Nonetheless, the slight improvement observed in group 1 could indicate the potential of CO_3Ap to enhance the compressive strength of the cement when combined with other materials, such as Si-CaP and $\text{Ca}(\text{OH})_2$, as observed in Group 2. Overall, the results demonstrate that incorporating Si-CaP and $\text{Ca}(\text{OH})_2$ did not universally improve the compressive strength of CO_3Ap cement. Only Group 2 showed a significant enhancement, while Groups 3–5 resulted in a loss of compressive strength.

3.2. SEM-EDS Analysis

In order to assess the bioactivity of the CO_3Ap cement, the formation of the apatite layer was observed using SEM. The SEM images showed that the apatite layer formation began with needle-like crystal growth in both the control and bioactivity specimens. Figure 2A,B show the surface of the control specimen before soaking in SBF, while Figure 2C,D depict the apatite crystal growth after one day of exposure to SBF. As expected, no crystal growth was observed on the control specimen before being exposed to SBF, as apatite formation requires the cement to be in contact with SBF. The SEM images demonstrate that the bioactivity specimen had a denser arrangement of apatite crystals than the control specimen after one day of exposure to SBF.

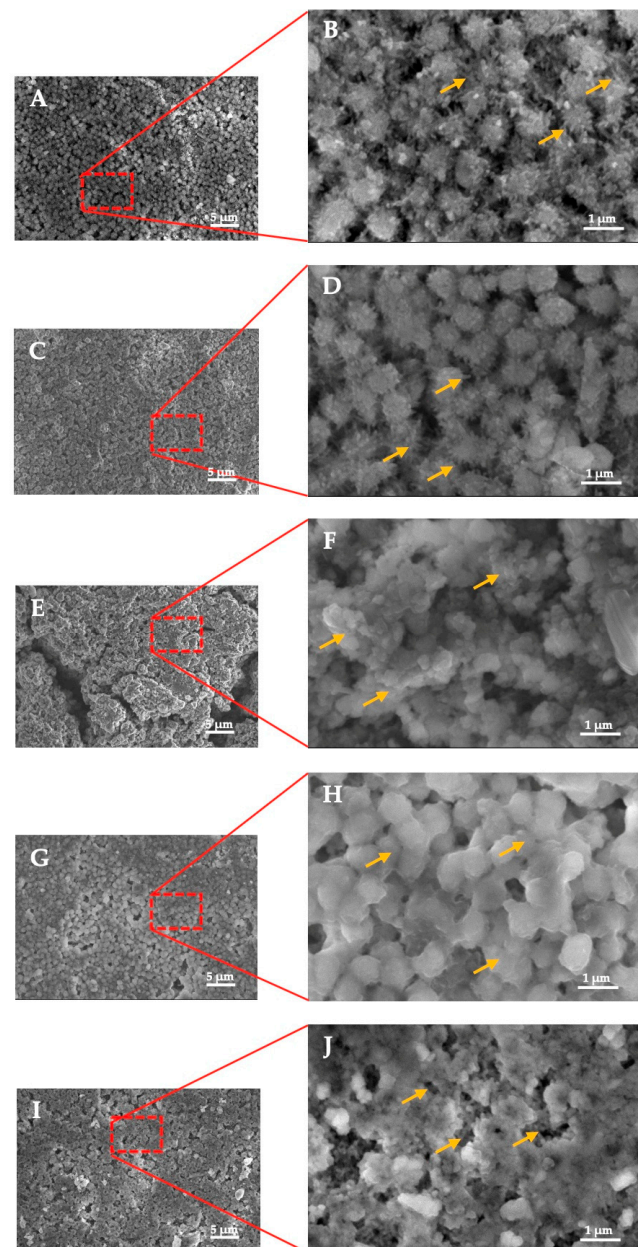


Figure 2. (A,B) control specimen; (C,D) 1-day exposure to SBF; (E,F) 7 days exposure to SBF; (G,H) 14 days exposure to SBF; (I,J) 21 days exposure to SBF. Noted: The red rectangle is the location of image magnification; the yellow arrow indicates the apatite crystal's growth and the apparent interface of the apatite layer.

After seven days of soaking in SBF, the apatite crystal growth was faster in both specimens, as shown in Figure 2E,F. However, the arrangement of the apatite crystals was less regular than in Figure 2C,D. The irregular crystal structure of the apatite formed due to multiple crystal growth mechanisms and the transformation of calcium phosphate [21] can explain this phenomenon. Figure 2G,H show that the apatite crystal fragments were still merging and not yet conjugated.

Finally, after 21 days of SBF exposure, the cross-section SEM revealed that the apatite layer grew denser and more homogeneous (Figure 2I,J). However, the formation of the apatite layer was not uniform across the surface, as evidenced by the black regions in the SEM images. There was no obvious interface, and the growth of the apatite layer depended on the extended soaking period.

Figure 3 summarizes the elemental component of set $\text{CO}_3\text{Ap-Si-CaP-Ca(OH)}_2$ cement after being soaked into SBF in four different periods of exposure (1, 7, 14, 21 days) that were analyzed using EDS. The measured area was 30 microns in diameter and located at the specimen's center. The mass% of Ca element increased over time. The average mass% of Ca element was 17.34%. The most significant increase in Ca element mass% was 18.55%, which occurred both before and after the specimens were soaked in SBF. In this study, the average P element mass% was 6.67%, and the most significant increase in P element mass% was 8.83%, which occurred between 14–21 days of soaking. However, the P element mass% did not exhibit a constant upward trend as the graph of Ca element. The mass% of P element decreased in one day and 14 days, respectively. In the case of Si, the average Si element was 4.45%, and the highest Si element concentration was 7.82% after 21 days of soaking.

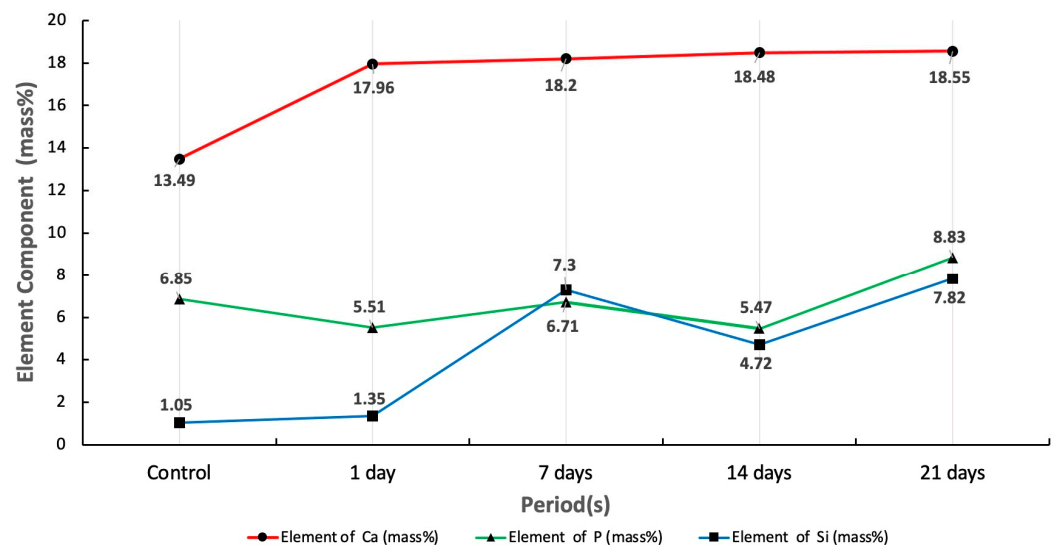


Figure 3. Evaluation of Ca, PO and Si elements before and after soaking into SBF for 1, 7, 14, and 21 day(s).

3.3. FTIR Analysis

The FTIR spectra of the set cement are summarized in Figure 4. FTIR analysis revealed that all specimen spectra differ before and after soaking in SBF. The CO_3^{2-} bands were detected at $863\text{--}879\text{ cm}^{-1}$ and $1427\text{--}1445\text{ cm}^{-1}$ in all specimens. In addition, the P-O symmetric stretch was also seen at $1027\text{--}1040\text{ cm}^{-1}$. These bands indicated CO_3^{2-} and PO_4^{3-} ionic substitution with the apatite structure. Due to the incorporation of Si-CaP, the spectra of set cement additionally showed the Si-O-Si vibration bands at 465 cm^{-1} and 1107 cm^{-1} .

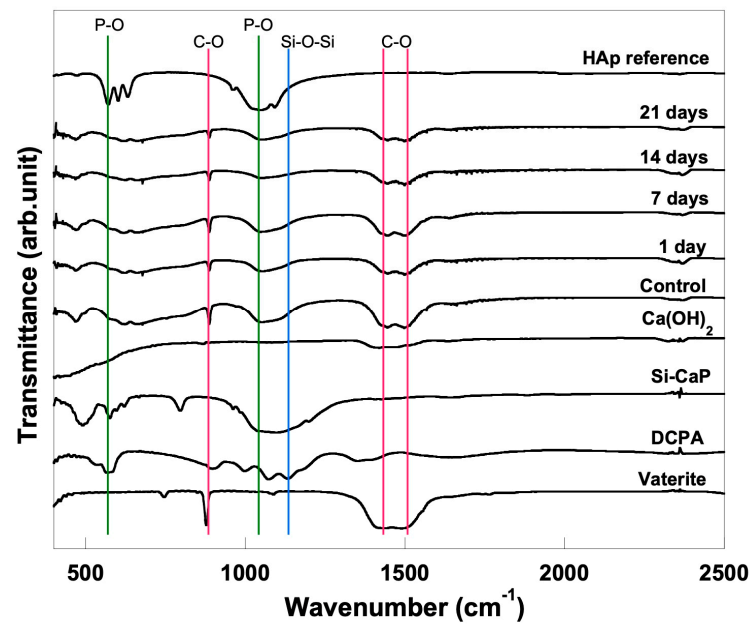


Figure 4. FTIR spectra of $\text{CO}_3\text{Ap-Si-CaP-Ca(OH)}_2$ set cement before and after soaking into SBF for 1, 7, 14, and 21 day(s).

3.4. XRD Analysis

The XRD spectra analysis (Figure 5) revealed that the control and bioactivity specimens underwent a phase transformation over time. The vaterite peaks in the range of $2\theta = 27.1\text{--}27.3$, $32.9\text{--}33.1$, and $43.5\text{--}43.7$ progressively decreased with increasing SBF soaking time, indicating the dissolution of the vaterite phase. Meanwhile, the peaks corresponding to an HA-like phase appeared and increased in intensity over time in the range of $2\theta = 26\text{--}26.1$ and $32\text{--}32.04$. After seven days of soaking, the vaterite peaks disappeared completely from the XRD spectra, and the presence of the HA-like phase was dominant. These results demonstrate that the CO_3Ap cement is capable of undergoing a phase transformation to form an apatite phase in both the control and bioactivity specimens over time.

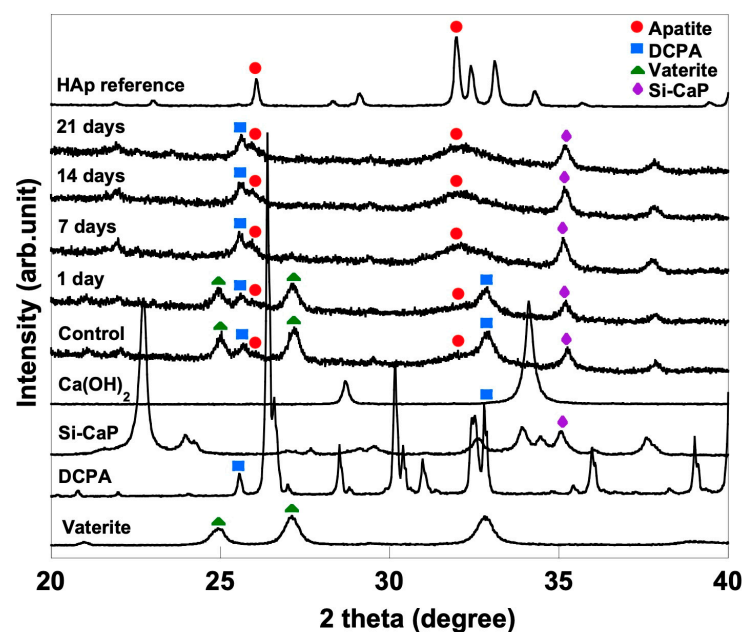


Figure 5. XRD patterns of $\text{CO}_3\text{Ap-Si-CaP-Ca(OH)}_2$ set cement before and after soaking into SBF for 1, 7, 14, and 21 day(s).

4. Discussion

Our previous study demonstrated that 40% vaterite and 60% DCPA mixed with various sodium phosphate solutions fully transformed to CO_3Ap with good osteoconductivity. However, the mechanical strength of the cement still needs to be improved to gain good clinical application [19]. In this investigation, 7% $\text{Ca}(\text{OH})_2$ and 3% Si-CaP improved the compressive strength and showed good bioactivity. However, it is important to note that the cement with the additives above has good bioactivity but is not necessarily enhanced. It is well established that the Si-CaP possesses advantageous physiochemical and bioactivity features [22]. When DCPA, vaterite, and $\text{Ca}(\text{OH})_2$ were mixed with the 0.2 mol/L of Na_2HPO_4 , the powder dissolved and supplied Ca^{2+} , PO_4^{3-} , and CO_3^{2-} ions. These ions became supersaturated and precipitated into CO_3Ap .

On the other hand, Si-CaP contributes to forming a network; the Si-OH from Si-CaP binds calcium supplied by DCPA, vaterite, and $\text{Ca}(\text{OH})_2$, forming a more dense structure, thereby increasing the compressive strength of this set cement. Additionally, incorporating Si-CaP into the cement has been shown to increase its compressive strength, making it a better option for clinical use. This is because the advantageous properties of Si-CaP not only enhance the mechanical properties of the cement, but also improve its bioactivity, making it more biocompatible and suitable for use in the body.

The ability of a material to cause a particular biological response is referred to as its bioactivity [23,24]. This response includes the production of hydroxyapatite layers on tissue surfaces. In vitro bioactivity evaluation helps determine whether a new bioactive substance can form bonds between tissue and material and serves as preliminary research for tests performed in vivo [20].

Our study showed that despite no exposure to SBF, the needle-like apatite crystal growth surrounding the globular structure can still be observed. A dissolution-precipitation reaction may be seen here, as evidenced by the interlocking of the precipitated apatite crystal structure [21,25,26]. The CO_3^{2-} , Ca^{2+} , and PO_4^{3-} ions dissolved and precipitated to form CO_3Ap crystals. Later on, the CO_3Ap precipitates and interlock with one another to form a more compact CO_3Ap arrangement [2].

As a result of contact between the CO_3Ap -Si-CaP- $\text{Ca}(\text{OH})_2$ cement with body fluid (in this study SBF), a dissolution-precipitation process took place as observed in the formation of the apatite layer (Figure 2C,D). The following describes each of these chemical steps: (1) surface de-alkalization exchange with H^+ , which leads to an increase in the local pH; (2) formation of $\text{Si}(\text{OH})_4$; (3) re-polymerization of $\text{Si}(\text{OH})_4$ to form SiO_2 rich layer; (4) precipitation of Ca and P ions; and (5) crystallization of $\text{CaO-P}_2\text{O}_5$ layer to form crystalline apatite structures [23,27].

The transformation of calcium phosphate into apatite resulted from numerous crystal growth mechanisms and the reconstruction of apatite crystals [28]. This corresponded to the irregular arrangement of apatite crystal, which emerged after seven days of soaking in SBF. With a longer SBF exposure time, the crystal arrangement of the apatite becomes denser. However, this arrangement does not appear to have formed uniformly across the surface of the specimen, even after it was subjected to SBF for 21 days. Apatite layer development shows evidence of an apparent dark non-collagenous interfacial zone (Figure 2G,H). The presence of an interfacial zone is consistent with previous studies showing the formation of the apatite layer [29,30]. Apatite crystals were formed by apatite precipitation in an aqueous solution at physiological pH and room temperature [31].

FTIR and XRD analyses provide evidence that apatite crystals are present. FTIR evaluation verifies the presence of C-O bands and a P-O symmetric stretch, which point to the ionic substitution of CO_3^{2-} and PO_4^{3-} within the apatite structure. In line with the FTIR results, the XRD result confirmed that apatite increases with the overexposure time of SBF. The rising Ca and P element is another essential indicator in bioactivity evaluation. Before and after soaking the specimen in SBF, there was an increase in the Ca element mass% that ranged from 13.49% to 18.55%. Besides Ca ions, P and Si ions contribute to

mineralised tissue regeneration and induce odontogenic differentiation to form dentinal bridge formation [8].

This study employs Si-CaP and Ca(OH)₂ to improve the compressive strength and shows good bioactivity of CO₃Ap cement but is still limited in scope and design. A limited number of variables were evaluated, and the timeframe over which the compressive strength and bioactivity of the CO₃Ap cement supplemented by Si-CaP and Ca(OH)₂ were assessed was short. In addition, the studies were performed on a microstructural level only, leaving out the macro- and micro-scale biological factors that govern the properties of the cement in the physiological environment. Therefore, there is a need to further study the effects of these additives of Si-CaP and Ca(OH)₂ on the in vitro and in vivo study of CO₃Ap cement.

5. Conclusions

The current study has demonstrated that incorporating Si-CaP and Ca(OH)₂ into CO₃Ap cement significantly enhances its compressive strength. Furthermore, the resulting CO₃Ap- Si-CaP -Ca(OH)₂ cement exhibits good bioactivity, as evidenced by apatite formation on its surface, as well as an observed increase in the average mass% of Ca, P, and Si elements, and the early formation of apatite crystals following immersion in the SBF solution. Further studies incorporating a control group are necessary to confirm its enhanced bioactivity. Overall, our findings suggest that CO₃Ap- Si-CaP -Ca(OH)₂ cement is a promising biomaterial for use in bone and dental tissue engineering applications.

Author Contributions: Research concept and design (A.C. and E.K.); collection and assembly of data (M.L.); data analysis and interpretation (A.C., E.K. and M.N.Z.); writing the manuscript (A.C., M.L. and M.N.Z.); manuscript review (A.C., M.N.Z., E.K., K.A.S. and C.S.); critical revision of the manuscript (A.C., M.N.Z., K.A.S., C.S. and A.E.-G.); synthesis of Si-CaP used in this study (A.E.-G.). All authors have read and agreed to the published version of the manuscript.

Funding: This research was funded by a grant from The Directorate of Higher Education Republic of Indonesia and Padjadjaran University, Indonesia No. 1207/UN6.3.1/PT.00/2021 (A.C.).

Institutional Review Board Statement: Not applicable.

Informed Consent Statement: Not applicable.

Data Availability Statement: Not applicable.

Acknowledgments: The authors would like to appreciate the research support, services, and facilities of the Integrated Laboratory of Faculty of Dentistry, Padjadjaran University, Indonesia, and collaborative research with the Universiti Sains Malaysia, University of Illinois Chicago and the University of North Carolina in Charlotte, USA.

Conflicts of Interest: The authors declare no conflict of interest.

References

1. Dorozhkin, S.V. Calcium orthophosphate cements and concretes. *Materials* **2009**, *2*, 221–291. [[CrossRef](#)]
2. Zakaria, M.N.; Cahyanto, A.; El-ghannam, A. Calcium release and physical properties of modified carbonate apatite cement as pulp capping agent in dental application. *Biomater. Res.* **2018**, *22*, 35. [[CrossRef](#)] [[PubMed](#)]
3. Eliaz, N.; Metoki, N. Calcium phosphate bioceramics: A review of their history, structure, properties, coating technologies and biomedical applications. *Materials* **2017**, *10*, 334. [[CrossRef](#)]
4. Al-sanabani, J.S.; Madfa, A.A.; Al-sanabani, F.A. Application of calcium phosphate materials in dentistry. *Int. J. Biomater.* **2013**, *2013*, 876132. [[CrossRef](#)]
5. Zakaria, M.N.; Fitriani, N.; Pauziah, N.; Sabirin, I.P.; Cahyanto, A. Evaluation of carbonate apatite cement in inducing formation of reparative dentin in exposed dental pulp. *Key Eng. Mater.* **2017**, *758*, 250–254. [[CrossRef](#)]
6. Zakaria, M.N.; Cahyanto, A.; El-Ghannam, A. Basic properties of novel bioactive cement based on silica calcium phosphate composite and carbonate apatite. *Key Eng. Mater.* **2016**, *720*, 147–152. [[CrossRef](#)]
7. Huang, J. *Biology and Engineering Stem Cell Niches, Chapter 20 Design and Development of Ceramics and Glasses*; Elsevier: London, UK, 2017; pp. 315–329.
8. Xu, H.H.K.; Wang, P.; Wang, L.; Bao, C.; Chen, Q.; Weir, M.D.; Chow, L.C.; Zhao, L.; Zhou, X.; Reynolds, M.A. Calcium phosphate cements for bone engineering and their biological properties. *Bone Res.* **2017**, *5*, 17056. [[CrossRef](#)]

9. Cahyanto, A.; Restunaesha, M.; Zakaria, M.N.; Rezano, A.; El-Ghannam, A. Compressive strength evaluation and phase analysis of pulp capping materials based on carbonate apatite-SCPC using different concentration of SCPC and calcium hydroxide. *Key Eng. Mater.* **2018**, *782*, 15–20. [[CrossRef](#)]
10. Aniket; Young, A.; Marriott, I.; El-Ghannam, A. Promotion of pro-osteogenic responses by a bioactive ceramic coating. *J. Biomed. Mater. Res. Part A* **2012**, *100*, 3314–3325. [[CrossRef](#)]
11. Crovace, M.C.; Souza, M.T.; Chinaglia, C.R.; Peitl, O.; Zanotto, E.D. Biosilicate[®]—A multipurpose, highly bioactive glass-ceramic. In vitro, in vivo and clinical trials. *J. Non. Cryst. Solids* **2016**, *432*, 90–110. [[CrossRef](#)]
12. Sathorn, C.; Parashos, P.; Messer, H. Antibacterial efficacy of calcium hydroxide intracanal dressing: A systematic review and meta-analysis. *Int. Endod. J.* **2007**, *40*, 2–10. [[CrossRef](#)] [[PubMed](#)]
13. Wu, C.; Xiao, Y. Evaluation of the in vitro bioactivity of bioceramics. *Bone Tissue Regener. Insights* **2009**, *2*, 25–29. [[CrossRef](#)]
14. Sanz, J.L.; Rodríguez-Lozano, F.J.; Llana, C.; Sauro, S.; Forner, L. Bioactivity of bioceramic materials used in the dentin-pulp complex therapy: A systematic review. *Materials* **2019**, *12*, 1015. [[CrossRef](#)] [[PubMed](#)]
15. Abbasi, Z.; Bahrololoom, M.E.; Shariat, M.H.; Bagheri, R.A. Bioactive glasses in dentistry: A review. *J. Dent. Biomater.* **2015**, *2*, 1–9.
16. Shibata, H.; Yokoi, T.; Goto, T.; Kim, I.Y.; Kawashita, M.; Kikuta, K.; Ohtsuki, C. Behavior of hydroxyapatite crystals in a simulated body fluid: Effects of crystal face. *J. Ceram. Soc. Jpn.* **2013**, *12*, 807–812. [[CrossRef](#)]
17. Kokubo, T.; Yamaguchi, S. Simulated body fluid and the novel bioactive materials derived from it. *J. Biomed. Mater. Res. Part A* **2019**, *107*, 968–977. [[CrossRef](#)]
18. El-Ghannam, A. Advanced bioceramic composite for bone tissue engineering: Design principles and structure bioactivity relationship. *J. Biomed. Mater. Res. Part A* **2004**, *69*, 490–501. [[CrossRef](#)]
19. Cahyanto, A.; Maruta, M.; Tsuru, K.; Matsuya, S.; Ishikawa, K. Fabrication of bone cement that fully transforms to carbonate apatite. *Dent. Mater. J.* **2015**, *34*, 394–401. [[CrossRef](#)]
20. *BS ISO 23317:2014; Implants for Surgery—In Vitro Evaluation for Apatite-Forming Ability of Implant Materials*. BSI Standards Publication: London, UK, 2014; pp. 1–24.
21. Cahyanto, A.; Tsuru, K.; Ishikawa, K. Carbonate apatite formation during the setting reaction of apatite cement. *Adv. Bioceram. Porous Ceram. V* **2010**, *3*, 147–164.
22. Gupta, G.; Kirakodu, S.; White, D.; El-Ghannam, A. Dissolution kinetics of a Si-rich nanocomposite and its effect on osteoblast gene expression. *J. Biomed. Mater. Res. Part A* **2006**, *80*, 486–496. [[CrossRef](#)]
23. Najdanović, J.; Rajković, J.; Najman, S. Bioactive biomaterials: Potential for application in bone regenerative medicine. In *Biomaterials in Clinical Practice: Advances in Clinical Research and Medical Devices*, 1st ed.; Zivic, F., Affatato, S., Trajanovic, M., Schnabelrauch, M., Grujovic, N., Choy, K., Eds.; Springer International Publisher: New York, NY, USA, 2017; pp. 333–360.
24. Smith, A.J.; Duncan, H.F.; Diogenes, A.; Simon, S.; Cooper, P.R. Exploiting the bioactive properties of the dentin-pulp complex in regenerative endodontics. *J. Endod.* **2016**, *42*, 47–56. [[CrossRef](#)]
25. Daitou, F.; Maruta, M.; Kawachi, G.; Tsuru, K.; Matsuya, S.; Terada, Y.; Ishikawa, K. Fabrication of carbonate apatite block based on internal dissolution precipitation reaction of dicalcium phosphate and calcium carbonate. *Dent. Mater. J.* **2010**, *29*, 303–308. [[CrossRef](#)]
26. Tsuru, K.; Yoshimoto, A.; Kanazawa, M.; Sugiura, Y.; Nakashima, Y.; Ishikawa, K. Fabrication of carbonate apatite block through a dissolution-precipitation reaction using calcium hydrogen phosphate dihydrate block as a precursor. *Materials* **2017**, *10*, 374. [[CrossRef](#)] [[PubMed](#)]
27. Lin, K.S.K.; Tseng, Y.H.; Mou, Y.; Hsu, Y.-C.; Yang, C.-M.; Chan, J.C.C. Mechanistic study of apatite formation on bioactive glass surface using ³¹P solid-state NMR spectroscopy. *Chem. Mater.* **2005**, *17*, 4493–4501. [[CrossRef](#)]
28. Lotsari, A.; Rajasekharan, A.K.; Halvarsson, M.; Andersson, M. Transformation of amorphous calcium phosphate to bone-like apatite. *Nat. Commun.* **2018**, *9*, 4170. [[CrossRef](#)] [[PubMed](#)]
29. Grandfield, K.; Palmquist, A.; Engqvist, H.; Thomsen, P. Resolving the CaP-bone interface: A review of discoveries with light and electron microscopy. *Biomatter* **2012**, *2*, 15–23. [[CrossRef](#)] [[PubMed](#)]
30. Rivera, E.M. Hydroxyapatite-based materials: Synthesis and Characterization. In *Biomedical Engineering-Frontiers and Challenges*, 1st ed.; Fazel-Rezai, R., Ed.; Intech: Rijeka, Croatia, 2011; pp. 75–96.
31. Vandecandelaere, N.; Rey, C.; Drouet, C. Biomimetic apatite-based biomaterials: On the critical impact of synthesis and post-synthesis parameters. *J. Mater. Sci. Mater. Med.* **2012**, *23*, 2593–2606. [[CrossRef](#)]

Disclaimer/Publisher's Note: The statements, opinions and data contained in all publications are solely those of the individual author(s) and contributor(s) and not of MDPI and/or the editor(s). MDPI and/or the editor(s) disclaim responsibility for any injury to people or property resulting from any ideas, methods, instructions or products referred to in the content.